

Modelling preferential transport

Frank Stagnitti

Centre for Applied Dynamical Systems & Environmental Modelling, Deakin University,
Geelong, Victoria, Australia 3217

Mathematical and computer-simulation models are widely used in Soil Physics and Hydrology for predicting water percolation and water-aided transport of solutes and contaminants through the unsaturated zone. However, discrepancies between model results and actual field measurements are commonly found in the literature. In spite of the many experimental findings, the preferential flow phenomena has not been adequately incorporated into simple mathematical models for predicting moisture and solute flow in the unsaturated zone. The major difficulty of modelling this transport phenomena is primarily due to characterising the flow-paths within the soil profile. The approach to predict water and solute transport is derived from the work of Richard's who formulated a theory of water movement in unsaturated soils (Richards, 1931). Van der Molen (1956) combined aspects of Richards' model with the theory of dispersive movement to predict desalinisation of land that had been inundated by seawater in the Netherlands. The resulting equation, the Convection-Dispersion equation (CDE), assumes that water and solutes follow an *average* path through the soil. Others (e.g., Parker and Van Genuchten, 1984; Sposito and Jury, 1988 and Barry and Sposito, 1988), have improved the solute transport model by incorporating a stochastic description of soil heterogeneities (see Barry, 1993; and Barry and Li, 1994 for excellent reviews). However, these results are usually limited to cases of constant or uniform mean velocity as well as constant dispersion (Gee, Kincaid, Lenhard, & Simons, 1991). Transfer function models have received considerable field testing and have shown that scale-dependent dispersion is present in the field (Li, Barry, Hensley, & Bajracharya, 1994; Li, Barry, & Stone, 1994). The conclusion from these studies is that the Convection-Dispersion equation with a constant dispersion coefficient does not give as great as solute dispersion with depth than is observed (Gee, Kincaid, Lenhard, & Simons, 1991).

Several more-recent models separate matrix flow from macropore flow. These dual-porosity models (e.g., see Gerke and van Genuchten, 1993), typically write separate transport equations for each domain of flow (i.e., matrix and macropore). Mixing of water and solutes across the interface is permitted and described by transfer coefficients which are often functions of the pore-size.

Steenhuis, Parlange, & Andreini, 1990 followed a similar conceptual framework and proposed a mathematical model that considers not two domains but any number of domains. Extensions and improvements to the model were later proposed by (Steenhuis, Nijssen, Stagnitti, & Parlange, 1991) and (Stagnitti, Steenhuis, Parlange, Nijssen, & Parlange, 1991). In any modelling attempt, characterisation of the soil profile is problematic. In the model proposed by Steenhuis and colleagues, preferential flow paths are simulated by taking piece-wise linear approximations of the hydraulic conductivity; resulting in two model parameters; N , the number of pore groups with mobile water and, v_p , the transport velocity of each pore group. These parameters can be related to physical properties but they usually require calibration to a particular field or laboratory experiment. Unlike the usual modelling assumptions applied in the Convection-Dispersion equation, the concentration of solutes in the percolating water is dependent on

the varying rate of applied water and the time period between rainfall and chemical application. This is achieved by relating the solute flux to the water flux. Thus transient field conditions can be simulated. The model can be applied to both large-scale field experiments and small-scale laboratory experiments.

Water and solutes may travel through a soil by any number of possible routes and at differing velocities. Thus the residence times of water-soluble contaminants in the vadose zone is highly variable. However, for the purposes of modelling, even though these paths may be highly distributed throughout the soil, they may be collected into groups of pathways or ‘capillary-bundles’ in which the moisture and solutes travel with approximately the same flux. These ‘capillary-bundles’ are also termed ‘pore-groups’. The total amount of moisture, $\theta(x,t)$ in the soil at time, t , and point, x , is the sum of all individual moisture contents for each capillary-bundle, p .

$$\theta(x,t) = \sum_{p=0}^N \theta_p(x,t) \quad (1)$$

where θ_p is the individual moisture content for the p^{th} pore-group. The maximum amount of moisture that each group can hold and transmit is $\Delta M_p = M_p - M_{p-1}$ where M_p and M_{p-1} are various moisture contents representing upper and lower limiting values for the p^{th} group and are a function of the size of pores in each group. When $\theta_p = \Delta M_p$, then all the pathways for the p^{th} group are completely saturated with soil moisture. The soil is locally saturated when all flow paths in all groups are saturated, ie. $\theta(x,t) = \theta_s$ and $\theta_p(x,t) = \Delta M_p$ for all p where θ_s is the saturated moisture content of the soil. The group’s moisture content, θ_p , is a function of the vertical percolation rate, q_p , and the effects of precipitation, evapotranspiration and loss or gain of moisture from interactions and exchanges with other groups. Therefore, from continuity, the transport equation may be written as

$$\frac{\partial[\theta_p(x,t)]}{\partial t} + \frac{\partial[q_p(x,t)]}{\partial x} = A_p(x,t) \quad (2)$$

for $t \geq 0$; $x \geq 0$; $0 \leq \theta_p \leq \Delta M_p$; $p = 0 \dots N$.

where $A_p(x,t)$ is a source/sink term representing the effects of precipitation, evapotranspiration and mixing between other groups; t is time, and x is a distance with $x = 0$ being the soil surface; N is the number of mobile pore-groups. From consideration of Darcy’s law,

$$\begin{aligned} q_p(x,t) &= k(\theta_p) H(x,t); & \text{for } p = 1 \dots N \\ q_0(x,t) &= 0 & \text{for } p = 0 \end{aligned} \quad (3)$$

and

$$0 \leq \theta_p \leq \Delta M_p; \quad q_0 \leq q_1 \leq q_2 \dots \leq q_N$$

where, $H(x,t)$ is the hydraulic gradient and $k(\theta_p)$ is the hydraulic conductivity. For moisture in the unsaturated zone, a unit gradient is assumed, i.e., $H(x,t) = 1$. This is a useful and accurate approximation when gravity is the main driving force and is appropriate for percolation in macropores (Parlange, Steenhuis, & Stagnitti, 1994). Therefore, after substitution

$$\frac{\partial \theta_p}{\partial t} + v_p \frac{\partial \theta_p}{\partial x} = A_p \quad \text{where} \quad v_p = \frac{dk(\theta_p)}{d\theta_p} \quad (4)$$

where v_p is the velocity of percolating moisture in the p^{th} group. Note that for $p = 0$, $v_p = 0$. The solution of eq. (9), obtained by the method of characteristics (e.g., see Charbeneau & Street, 1979; Charbeneau, 1981; Charbeneau, 1984), is given by

$$x = v_p t + x_0, \quad (5)$$

and

$$\theta_p(x,t) = \int_0^t A_p dt + \theta_p(x_0,0) \quad ; \quad x \geq v_p t \quad (6)$$

where $\theta_p(x_0,0)$ is an arbitrary function of x_0 when $t = 0$. Eq. (11) cannot be easily integrated because A_p is generally not a simple analytical expression. Therefore, a fixed time-step numerical solution for the moisture content θ_p was proposed. From eq. (15), in a small time interval, Δt , moisture will travel a distance, Δx_p , given by

$$\theta_p(x,t) = \theta_p(x - \Delta x_p, t - \Delta t) + I_p(x,t); \quad \Delta x_p = v_p \Delta t \quad (7)$$

where I_p is the integral of A_p between $(t - \Delta t)$ and t . Let Δx_p be a simple integer multiple γ_p of Δx_1 , the distance travelled by moisture in the slowest moving group ($p = 1$), i.e., $\Delta x_p = \gamma_p \Delta x_1$ with $\gamma_1 = 1$. Note that in the “smaller” time step $(\Delta t / \gamma_p)$, the p^{th} group moved a distance Δx_1 . Therefore, define a grid of points in $(x-t)$ space based on Δx_1 and $(\Delta t / \gamma_T)$ where $T = N + 1$, is the label for the pore-group with the greatest flux. Then

$$x = i \Delta x_1; \quad i = 0, 1, 2 \dots L / \Delta x_1 \quad \text{and} \quad t = j (\Delta t / \gamma_T); \quad j = 0, 1, 2 \dots \quad (8)$$

where L is the depth to groundwater. On this grid, only one parameter, either the spatial coordinate, Δx_1 or the time coordinate $(\Delta t / \gamma_T)$ needs to be specified.

It is usually more convenient to fix the time rather than the distance and therefore the following equation for moisture transport results.

$$\theta_p^{(i,j)} = \theta_p^{(i - \delta_p \gamma_p, j - 1)} + I_p^{(i,j)} \quad (9)$$

where

$$\delta_p = \begin{cases} 0 & ; \quad j \bmod \gamma_p \neq 0 \\ 1 & ; \quad j \bmod \gamma_p = 0 \end{cases}$$

Fig. 1. illustrates the operation of the model defined as by eq. (9). In this example, suppose $N = 3$ (i.e., there are three mobile pore-groups, $p = 1, 2,$ and 3), one immobile pore group ($p = 0$) and one macropore group, ($p = 4$). The transport velocities for each pore group are summarised in Table 1.

Table 1. Pore velocities and transport coefficients for the example given in Fig. 1.

<i>Category</i>	<i>Pore Group Number</i> (p)	<i>Transport Coefficient</i> (γ_p)	<i>Pore Velocity</i> (cm/hr)
Immobile	0	1	0
Mobile	1	1	19.5
Mobile	2	2	39.1
Mobile	3	4	78.1
Macropore	4	64	1250

For this example, $\Delta t = 1$ minute. Therefore, the “small” time step as defined by eq. (7) is $(\Delta t / \gamma_T) = 1/64$ min, a little less than one second. The reason for maintaining a second “small” time step $(\Delta t / \gamma_T)$ in the model is to provide a uniform rate of mixing of water (and solutes) during Δt . (The mechanism of mixing water and solutes for each time step will be described shortly). The spatial step, $\Delta x_1 = 0.33$ cm. This is the distance moisture (and solutes) will move in the first pore-group in one minute. After one minute, moisture (and solutes) in the second, third and fourth pore-groups would have travelled a distance of $2\Delta x_1$ (0.66 cm), $4\Delta x_1$ (1.32 cm) and $64\Delta x_1$ (21.3 cm), respectively.

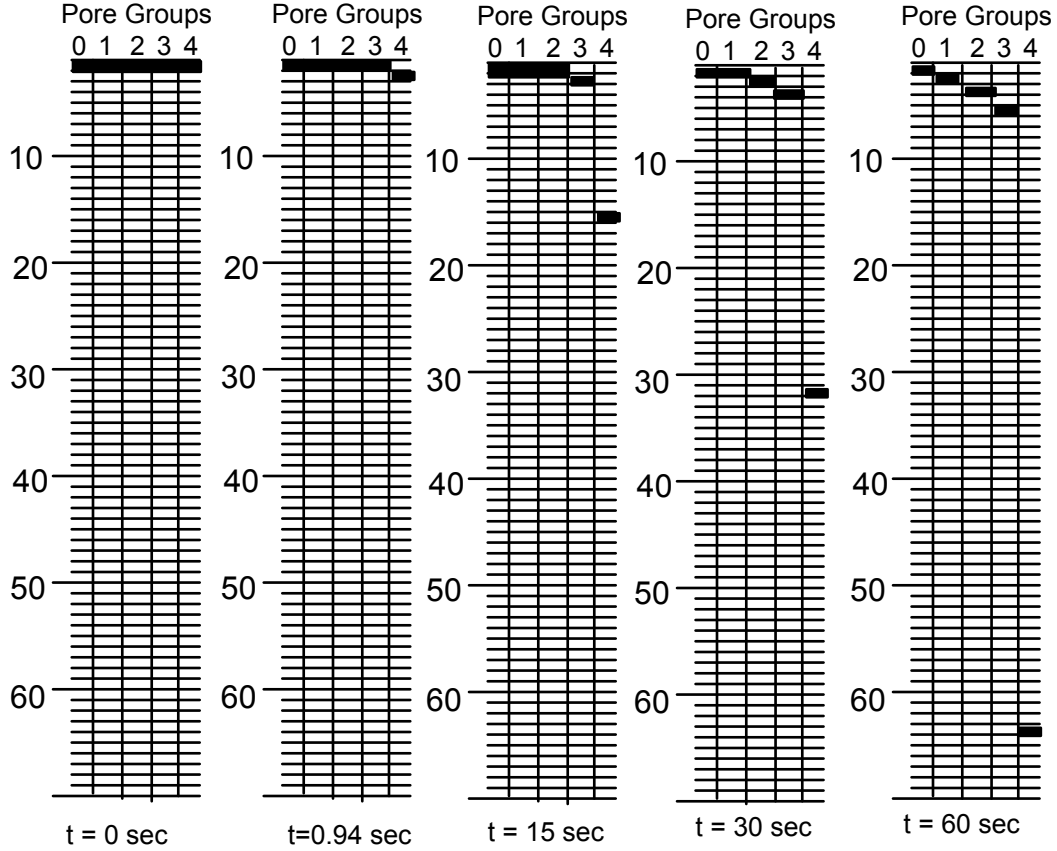


Figure 1. Transport of water and solutes in the preferential flow model (see eq. 8). The time step is defined by eq. (2). The spatial coordinate x is directed downward and the small divisions represent the space step Δx_1 (see eq. 8). (Adapted from Nijssen, Steenhuis, Kluitenberg, Stagnitti, & Parlange, (1991) .

Determining The Number Of Groups For A Soil

The total number of pore-groups, the amount of water in each group and its flux cannot be individually measured by experiments and generally will have to be estimated or determined by calibration. Indeed, it is difficult to conceive of an experiment that could determine such groupings. However, we propose a simple but general method for selecting any number of pore-groups for a soil based on a piece-wise linear approximation of the hydraulic conductivity function as shown in Fig. 2.

The derivation of the following equations is presented in Appendix A. The moisture content and conductivity for the p^{th} pore is given by,

$$M_p = \theta_r + (\theta_s - \theta_r) (1 - n) \left[\frac{f^{(a+1)(N-p)} (1 - f^{-a})}{1 - f} \right] \quad p = 1 \dots N - 1 \quad (10)$$

and

$$K_p = \left[\frac{k_s (1 - n)}{n} \right] \left[\frac{f^{a(N-p)} (f - f^{-a})}{1 - f} \right] \quad p = 1 \dots N - 1 \quad (11)$$

where, N is the number of pore groups with mobile water, $a = 1 / (n - 1)$ is a property of the soil and n is the reciprocal exponent in the power law of the hydraulic conductivity function which depends on soil type (Brooks and Corey, 1964) given by

$$k(\theta) = k_s \left[\frac{\theta(x,t) - \theta_r}{\theta_s - \theta_r} \right]^{1/n} \quad (12)$$

where k_s is the saturated hydraulic conductivity, θ_s is the moisture content at saturation. Note, equations (10) and (11) are valid for $p = 1 \dots N - 1$. For $p = N$, we have

$$M_N = \theta_s \quad \text{and} \quad K_N = k_s \quad (13)$$

and for $p = 0$, we have

$$M_0 = \theta_r + (\theta_s - \theta_r) (1 - n) f^{(a+1)(N-1)} \quad \text{and} \quad K_0 = 0 \quad (14)$$

Therefore, the velocity for each pore-group can be written as

$$v_p = k_s f^{(p-N)} / [n (\theta_s - \theta_r)] ; \quad p = 1 \dots N \quad (15)$$

and

$$\gamma_p = v_p / v_1 = f^{p-1} ; \quad \gamma_p \leq L / \Delta x_1 \quad (16)$$

Note, f is an integer greater than one (e.g., 2, 3, etc). If $f = 2$, for example, the velocity of the second pore group is twice as fast as the first and the velocity of the third is twice as fast as the second and so on. If $f = 3$, then the velocity of the second pore group is three times faster than the first, etc (e.g., see Figs 1 and 2). Any soil may be simulated by selecting values for f and N .

Macropore Flow

The number of pore-groups, their limiting moisture contents and flux, can be linked to physically measurable parameters such as soil type and hydraulic conductivity. Any number of additional pore-groups representing flow through macropores and subsurface channels can be added to the model. The transport of moisture in macroporous groups is catered for in the same manner to the other pore-groups, i.e. by defining transport coefficients which are a simple integer multiple of the velocity of moisture in the slowest pore group.

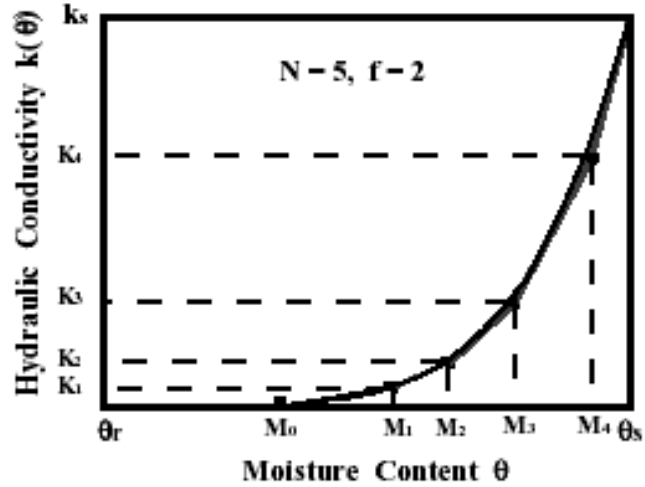


Figure 2. Piece-wise approximation to the unsaturated hydraulic conductivity function. Used to simulate pore-groups in the soil layer.

$$\gamma_p = v_p / v_1 \quad \text{for } p = N+1, N+2 \dots T \quad (17)$$

and where in this case, γ_p represents how much faster moisture in the p^{th} macropore group travels compared to moisture travelling in the slowest moving pore-group ($p = 1$). Although, in principle, any number of macropore groups can be modelled in this way, in practice it is hard to justify selecting any more than one macropore group without experimental evidence.

Solute Concentration

The solute concentration, $c(x,t)$, in the soil is given by

$$c(x,t) = \frac{s(x,t)}{\theta(x,t)} \quad (18)$$

where $s(x,t)$ is the total solute load given by

$$s(x,t) = \sum_{p=0}^T s_p^{(ij)} \quad (19)$$

and S_p is the solute mass in pore-group p . Assuming, for the moment, that chemical processes like adsorption and solute precipitation are negligible, then the solute flux may be simply written as

$$s_p^{(i,j)} = s_p^{(i-\delta_p, \gamma_p, j-1)} + \psi_p^{(i,j)} \quad (20)$$

where $\psi_p^{(i,j)}$ is the solute amount added to or subtracted from the p^{th} group during $\Delta t / \gamma_p$. In each time step the concentration of solutes in each group is affected by three processes: evapotranspiration (moisture extracted from the soil), precipitation (moisture entering the soil after infiltrating the soil surface) and mixing or interchange between capillary-bundles in order to attain chemical equilibrium. These three processes determine the value of $\psi_p^{(i,j)}$. Each process is described below. In the first step, moisture is extracted from each capillary-bundle or pore-group in the soil in various amounts as a result of evapotranspiration. Evapotranspiration also helps to redistribute moisture and consequently solutes between groups. Let $E^{(i,j)}$ represent the evapotranspiration loss from the soil at time j and depth i . Since this loss does not have to be uniform with depth nor with respect to the capillary bundle, let ξ_p represent the fraction of the total loss that was taken from group p during $\Delta t / \gamma_p$. If $\theta_p^{(i,j)}$ represents the moisture content just prior to accounting for evapotranspiration in the model, then the new moisture content after subtracting the evapotranspiration loss for the p^{th} group is given by

$$\theta_{p(E)}^{(i,j)} = \theta_p^{(i,j)} - \xi_p \frac{E^{(i,j)}}{D}; \quad \text{for } 0 \leq \xi_p \leq \theta_p^{(i,j)} D / E^{(i,j)} \quad (21)$$

where D is the depth to the root zone and the subscript E represents the new moisture content after evapotranspiration has been accounted for in the time step, j . Although the concentration is affected, the amount of solutes remains unchanged.

In the second step, the net precipitation (precipitation less interception) is distributed in the soil to the various capillary-bundles. Exactly how this distribution occurs in the soil is a complex process and depends on the infiltration rate and the moisture status of the soil. Since this distribution is often non-uniform, let μ_p represent the fraction of the total precipitation that is added to the p^{th} group following rain. Therefore,

$$\theta_{p(ER)}^{(i,j)} = \theta_{p(E)}^{(i,j)} + \mu_p \frac{P^{(i,j)}}{D}; \quad \text{for } 0 \leq \mu_p \leq \Delta M_p - \theta_{p(E)}^{(i,j)} D / P^{(i,j)} \quad (22)$$

where $P^{(i,j)}$ is the amount of precipitation at (i,j) and the subscript (ER) represents the new moisture content after accounting for evapotranspiration and precipitation. Let $C_R^{(i,j)}$ be the concentration of solute in the precipitation and let $s_p^{(i,j)}$ be the amount of solute in the group just prior to rain. Therefore, the amount of solute in the soil after rain is

$$s_{p(ER)}^{(i,j)} = s_p^{(i,j)} + \mu_p \frac{P^{(i,j)}}{D} (\Delta t / \gamma_T) C_R^{(i,j)} \quad (23)$$

where $s_{p(ER)}^{(i,j)}$ represents the amount of solutes in the p^{th} pore-group after accounting for precipitation.

The network of flow paths in the soil are interconnected. Therefore, in the final step, there is an exchange of moisture and solutes between the various capillary-bundles ranging from complete exchange of moisture and solutes to no exchange or mixing. Mathematically, this behaviour might be described by three strategies (a) complete mixing, (b) partial mixing, and (c) no exchange between pore-groups within the simulated time interval. These three strategies covering the continuum of possible behaviour should be implemented within the model. For example, under option (b), an appropriate partial mixing strategy might be one in which a substantial portion of the moisture and solutes in the slower pore-groups are exchanged within the time interval whereas for faster moving pore-groups or macropore groups, very little exchange occurs in the simulated time step (Skopp, Gardner & Tyler, 1981).

All strategies can be modelled easily by defining two sets of coefficients, $\lambda_p(\theta_p)$ and $\eta_p(\theta_p)$. Let λ_p represent the fraction of moisture extracted from group p and placed into a “common” pool ($0 \leq \lambda_p \leq 1$), and let η_p represent the fraction of the “common” pool that is moved back into the p^{th} group after mixing. After mixing, the new moisture content will be given by

$$\theta_{p(ERM)}^{(i,j)} = (1 - \lambda_p) \theta_{p(ER)}^{(i,j)} + \eta_p \sum_{g=0}^T \lambda_g \theta_{p(ER)}^{(i,j)} \quad (24)$$

The values for the mixing coefficients λ_p and η_p depend on the soil type and would normally have to be found by careful experimentation. In a similar fashion, after mixing is accounted for, we have

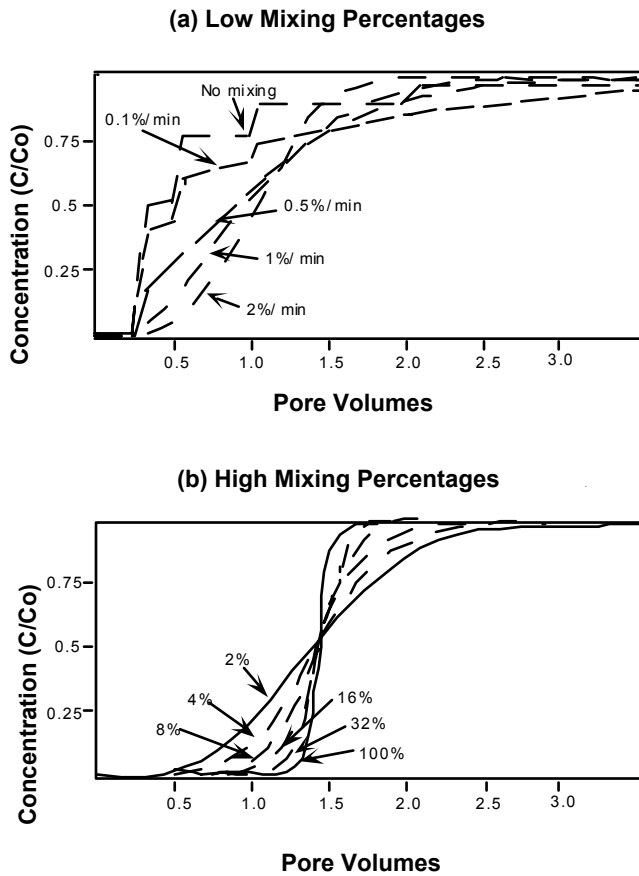
$$s_{p(ERM)}^{(i,j)} = (1 - \lambda_p) s_{p(ER)}^{(i,j)} + \eta_p \sum_{g=0}^T \lambda_g s_{p(ER)}^{(i,j)} \quad (25)$$

where $s_{p(ERM)}^{(i,j)}$ is the amount of solutes in group p after the mixing process has been accounted for and is equivalent to the right hand side of eq. (20) after the processes of evapotranspiration, precipitation and chemical mixing and interchange have been accounted for. There are certain conditions and restrictions on the range of values that the mixing coefficients can have. These are fairly obvious and result from consideration of the conservation of mass. In particular, if a set of coefficients for λ_p are adopted for a particular mixing strategy, then the values for η_p will be determined at each time step and depend on the amount of moisture in the pore group, the capacity of the pore-group to store additional moisture and the value of λ_p . Eqs (24) and (25) are bound by the following conditions

$$\sum_{p=0}^T \eta_p = 1; \quad \text{and} \quad \eta_p \leq \left[\Delta M_p - (1 - \lambda_p) \theta(\text{ER})_p^{(i,j)} \right] / \sum_{g=0}^T \lambda_g \theta(\text{ER})_g^{(i,j)} \quad (26)$$

Clearly, any number of mixing strategies can be adopted depending on the values for λ_p . For example, no mixing can be implemented by taking $\lambda_p = 0$ for all p . Partial mixing is simulated when $0 < \lambda_p < 1$ and full mixing occurs when $\lambda_p = 1$ for all p . A partial mixing strategy which tends to move moisture (and solutes) from pore-groups with small available moisture capacities (i.e., small ΔM_p) to groups with larger moisture capacities is given by

$$\eta_p = \left[\Delta M_p - (1 - \lambda_p) \theta(\text{ER})_p^{(i,j)} \right] / \sum_{g=0}^T \Delta M_g - (1 - \lambda_g) \theta(\text{ER})_g^{(i,j)} \quad (27)$$



Figures 3a and 24b. Influence of different mixing percentages on the breakthrough curves for a simulated soil column.

Other strategies were suggested by Stagnitti, et al., (1991). Fig. 3a and 3b illustrate the effects that different mixing strategies have on the breakthrough curves for a simulated soil column. For each simulation, the values for λ_p are the same for each pore group (eg. 2% per time step for all pore groups). Thus at the end of each time step, the concentration in each individual capillary-bundle or pore-group is

$$c_p^{(i,j)} = s_{p(\text{ERM})}^{(i,j)} / \theta_{p(\text{ERM})}^{(i,j)} \quad (28)$$

Comparison With The Convection - Dispersion Equation

Fig. 3 shows that the preferential flow model behaves like a Convection-Dispersion model when complete mixing is adopted and like a capillary-bundle model when no mixing is adopted. The breakthrough

curves were obtained for a hypothetical soil column by applying an instantaneous concentration of solute under steady-state flow conditions.

Hydrodynamic dispersion coefficients were fitted to the simulated breakthrough curves using CXT-FIT from Parker and van Genuchten (1984). Not surprisingly, the preferential flow model was found to behave very much like the Convection-Dispersion equation when saturated flow conditions and 100% mixing in all pore groups was adopted. Even under unsaturated flow conditions, the dispersion coefficient calculated using the input parameters from the preferential flow model was highly correlated with the fitted coefficients from CXT-FIT. Fig. 4 illustrates the relationship between the mixing coefficient, λ_p expressed and the fitted hydrodynamic dispersion coefficient for the Convection-Dispersion equation for a simulated soil column with an instantaneous concentration of solute under steady-state flow. Clearly, as expected, the mixing coefficients are inversely proportional to the hydrodynamic dispersion. Thus the Preferential Flow Model with the simple mixing strategies outlined above may be considered as an extension to the Convection-Dispersion equation.

Applications Of The Preferential Flow Model To Field And Laboratory Experiments

Application of the Preferential Flow Model to three different experiments is now illustrated. The first is a hillslope experiment conducted at the Cornell University's Turkey Hill Research Site near Ithaca, New York (Steenhuis and Muck, 1988). The plot is 23 m wide and 109 m long with an area of about 0.25 ha. The soil is a silt loam with a clay pan of compact till at 30 cm depth. The surface slope is a uniform 8%. A hay-grass mixture covered the plot. At the lower end of the plot both the volume and quality of the subsurface water and surface water were measured. A sprinkler irrigation system used water in a nearby creek to irrigate the plot. The outflow data for an experiment, carried out in December of 1978 in which nitrate-N and chloride-Cl was surface applied to saturated soil, is used here. The temperatures during this experimental period were just above freezing and consequently denitrification was extremely small. Evapotranspiration was negligible. The artificial precipitation averaged 0.6 cm/h and was maintained for over 80 hours. The amount of nitrate in the irrigated water was negligible but the concentration of chloride in the irrigation water ranged from 14 mg/l to 16 mg/l. Therefore, we took the initial

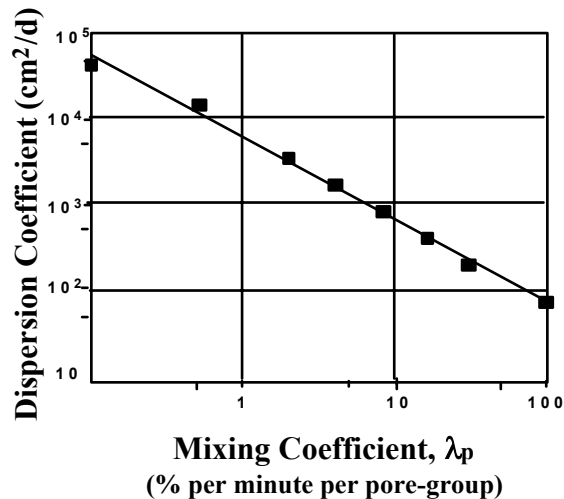


Figure 4. Relationship between the mixing coefficients for the Preferential Flow Model (λ_p) and the hydrodynamic dispersion coefficients obtained from CXT-FIT for a hypothetical soil column with and instantaneous application of solutes under steady state flow.

concentration of nitrate to be zero and that for chloride at 15 mg/l. Before applying the chloride and nitrate, steady state drainage conditions were achieved by irrigating for a 24 hour period. The average measured saturated conductivity was 12 m/d and saturated moisture content was 52.5%. A field capacity of 46% was reported by Steenhuis and Muck (1980). The residual moisture content was 0.0%.

The mathematical formulation presented in this paper was developed for vertical percolation through the soil. However, Stagnitti, et al., (1991) demonstrated that with very little modification to the mathematical formulation presented here, the preferential flow model could also be applied to hillslope experiments. The major changes to the model include modifying the flux for downslope transport and incorporation of surface runoff. The reader is referred to that paper for further details. The applied solutes were only added initially to the macropore and surface runoff groups and then allowed to mix slowly into the micropores and immobile pore-groups as experimental measurements indicated that when the chemicals were surface applied to the saturated soil, the chemicals did not mix readily with the immobile water (Richard and Steenhuis, 1988). For this experiment, we adopted the following: $f = 2$ and $N = 2$ (i.e., two mobile pore groups and one immobile group). We added two additional pore groups, one for surface runoff and the other a macropore group. The upper and lower moisture limiting values for the immobile pore group were 0 and 0.352 and for the mobile pore groups, they were (1) 0.353 and 0.485, and (2) 0.486 and 0.525. The upper and lower limiting moisture contents for the macropore group were 0.525 and 0.675 respectively. If the local moisture content after accounting for precipitation exceeded 0.675 at any time, then the additional moisture was added to the surface runoff group. We also adopted an initial moisture profile which is consistent with steady-state drainage with an irrigation rate of 0.6 cm/h. Water and solutes in the surface runoff moved at a rate 32 times faster than the slowest moving group. Therefore, γ_p equalled 1, 2, 4 and 32, respectively. The small time step was a quarter of an hour. This was similar to the time period in which measurements were taken. Therefore, $\Delta x_1 = 1.52$ m. How much of the solutes should be blended per time step? There is no *a priori* method of determining this. Four possibilities for λ_p . The first was no mixing, i.e., $\lambda_p = 0\%$ for all p . In subsequent trials we took 2%, 5% and 10% solutes blended per quarter hour per group.

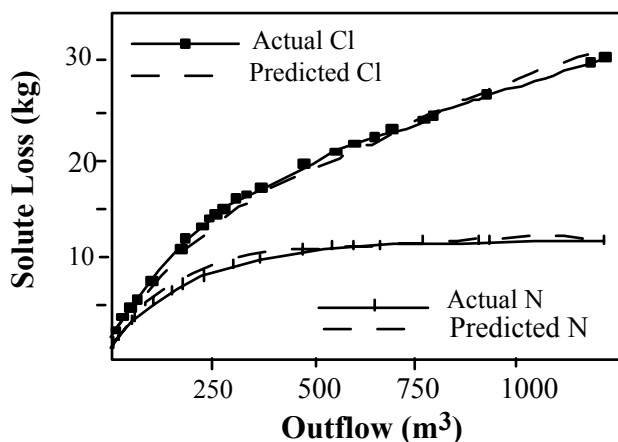


Figure 5. Predicted solute loss (broken lines) using the preferential flow model plotted with observed loss (solid lines) for application of chloride (squares) and nitrate (crosses).

narrower. The second example of the application of the model is illustrated in Fig. 6. The Preferential Flow Model was applied to a series of experiments conducted on undisturbed soil cores by Anderson and Bouma in 1977. Anderson and Bouma (1977a and b) conducted a series of laboratory experiments to determine the dispersion coefficients for soils consisting of blocky and coarse prismatic structures. In these experiments, three similar columns were subject to four different flow treatments using chloride as a tracer. Each soil core was 10 cm in diameter and the length ranged from 43 to 52 cm. Three replications of each experiment were studied. The first two experiments examined saturated flow conditions. The columns were initially saturated with water and then a 300 ppm solution of potassium chloride was ponded on the top of each column at shallow depth (Experiment 1). After the effluent concentration reached the input concentration, the columns were then flushed with water and drained leaving the larger pores filled with air. Another continuous dose of 300 ppm of chloride concentration was applied by ponding (Experiment 2). This was then followed by another flushing and draining and then a pulse application of 1 cm per day irrigation by ponding (Experiment 3). The final experiment consisted of ponding water on a gypsum crust giving a steady, continuous infiltration of approximately 1 cm/d (Experiment 4). Steenhuis, et al., (1991) and Nijssen, et al., (1991) analysed these experiments by conducting two simulations. For the first simulation, $N = 7$ (i.e., seven mobile pore groups) and $f = 2$. The velocity v_p of the slowest moving group was 1.85 cm/d and the fastest pore-group was 118.6 cm/d. The simulation time step was 3 minutes and solutes were blended at the following rates $\lambda_p = 0, 0.1, 0.15, 0.5, 0.75, 1.5, 1.75, \text{ and } 2.0$ % per 3 minutes. Although the mixing coefficients were large for the larger pore-groups, the overall mixing in the small pores is greater due to the longer retention time of solutes in those pores. In the second simulation, only the shape of the hydraulic conductivity function was modified by making the fastest moving pore-group transport water and solutes at a rate 256 times faster than the slowest moving pore-group rather than 64 times as in simulation 1 (i.e., a factor of 4) and thus enhancing macroporous flow. All other parameters remained

In each case, values for η_p were chosen to conserve mass (see Stagnitti, et al., (1991) for further details). The case for 2% gave the best fit and is presented in Fig. 5. The predicted solute loss for both chloride and nitrate is in very good agreement with the observed loss. It is indeed remarkable that the one set of parameters fit both data sets extremely well. However, this experiment alone may not be very convincing given the number of degrees of freedom the model has for parameter estimation. The following two sets of laboratory experiments further illustrates the applicability of the model but in these cases the range of values that the parameters may adopt is much

unaltered. The predicted breakthrough curves for the two simulations plotted with the observed breakthrough curves are presented for each of the four experiments in Fig. 27.

The range of values for the observed breakthrough curves provides an indication of the experimental variation between the columns. In all cases, except for Experiment 2, the predicted breakthrough curves for both simulations fell within the range of observed values. For Experiment 3, the predicted pulse application showed large variation within a day. These were not observed in the original data set because the concentrations were only measured daily whereas our model simulations were conducted on a 3-minute interval. If we averaged our predicted concentrations on a daily basis a very similar breakthrough curve would result. The second experiment clearly shows the significant effect of macropore flow on the breakthrough curve. The almost instantaneous response in the effluent concentration was attributed by Anderson and Bouma to flow through the larger air-filled pores. Our second simulation which enhanced the effect of the macropore flow more closely matched the observed values than the first simulation. It is very difficult to match the breakthrough curves for Experiments 1 and 2 with the same hydraulic conductivity function. It is likely that different conductivity functions for drained columns and saturated columns should be applied due to swelling of the soil and consequent narrowing of the cracks and voids (Steenhuis, et al., 1991). The model, however, was able to simulate a wide variety of breakthrough curves without changing other physical properties of the soil. In contrast, Anderson and Bouma tried to fit dispersion coefficients to the experiments using the Convection-Dispersion equation but found that the coefficients varied considerably and were highly dependent on the flow regime.

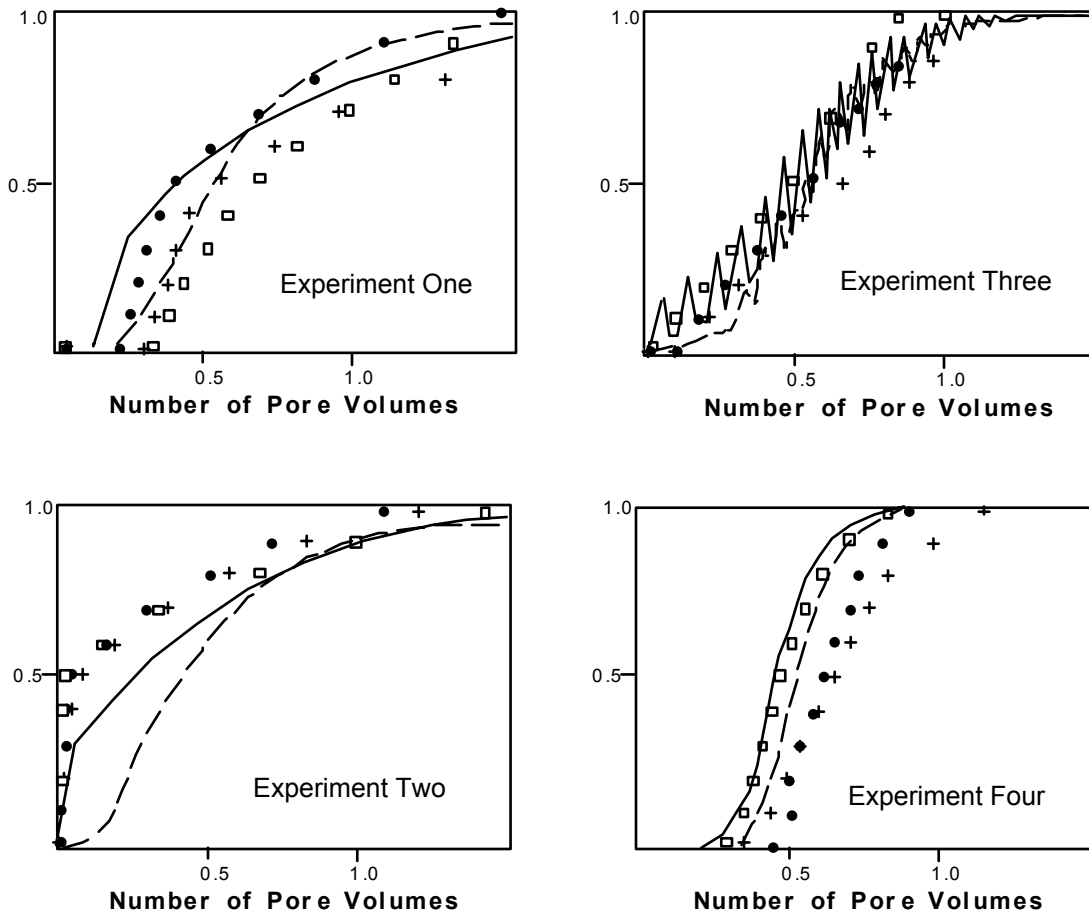


Figure 6. Predicted and observed breakthrough curves for the Anderson and Bouma, 1977a and 1977b data. The solid lines represent model predictions for the second simulation and the dashed lines represent model predictions for the first simulation. The symbols (squares, pluses and asterisks) represent the observed data for three different replications (soil columns).

In more recent experiments conducted by Kluitenberg and Horton (1990), three undisturbed soil cores containing macropores were taken from the A horizon of a glacial-till comprising of a fine loam mix. Each column had a diameter of 18 cm and lengths of 33, 33 and 35 cm. Labelled A, B and C, the columns had saturated hydraulic conductivities ranging from 58, 28 to 12 cm/h respectively and an average saturated moisture content of 0.44. At the beginning of the experiment, all columns were saturated for a 12 h period with a 0.01 N solution of calcium sulphate solution. Then, a 0.05 N solution of calcium chloride solution was ponded with a constant head on each column (Experiment 1). After about two pore volumes of this solution had infiltrated, the columns were extensively leached with the 0.01 N solution of calcium sulphate solution and then allowed to drain for a further 12 hour period. Next, 200 ml of a 0.05 N solution of calcium chloride solution was applied to the surface as a pulse (Experiment 2).

Once this solution had infiltrated, a 0.01 N solution of calcium sulphate solution was ponded on the surface and leached and drained once more. Then, an application of a 0.25 N solution of calcium chloride solution was dripped on the surface during a 6 to 8 minute

interval during which no ponding occurred (Experiment 3). After 15 minutes, the columns were again ponded with the calcium sulphate solution.

For these experiments, four mobile pore-groups and an immobile pore group were selected and the velocities of solute and moisture flow for the mobile pore groups were 19.5, 39.1, 78.1 and 1250 cm/h respectively; the latter representing macroporous transport (see Table 1). The “small” time step was 1/64 mins. Mixing was facilitated by blending approximately 0.8% of solutes in the immobile group and 0.004% of solutes in the mobile pore-groups in each time step (Nijssen, et al., 1991). Once again, this strategy results in more mixing in the slower moving groups than the faster ones due to the longer residence times in the soil. All other input parameters such as flow rates, duration of chloride pulse, initial moisture status etc. were determined from the actual data. Figures 7, 8 and 9 illustrate the simulated and observed breakthrough curves for columns A, B, and C. Since Kluitenberg and Horton (1990) observed that air entrapment caused variation in the flow rate, the concentrations of the effluent are plotted against pore volume. Figures 7a, 8a and 9a show breakthrough curves for each column for the first experiment where the chloride was ponded at the surface of the soil for approximately two pore volumes. The model reasonably predicts the observed data except for the initial breakthrough. The most remarkable feature for the observed and predicted breakthrough curves is the difference between the pulse and drip applications (Experiments 2 and 3) which are shown in figures 7b, 8b and 9b. For the drip application, the column remained unsaturated, whilst for the pulse, the solution was applied in a single slug. The resulting breakthrough curves are quite different as one might expect. For all columns, the pulse application resulted in a sharp, early peak whilst for the drip experiment, the breakthroughs were smaller and the peak arrived later. The model, without changing the soil and solute properties, was able to predict these differences quite well. Therefore, unlike the Convection-Dispersion equation, the model is sensitive to the rate of effluent application.

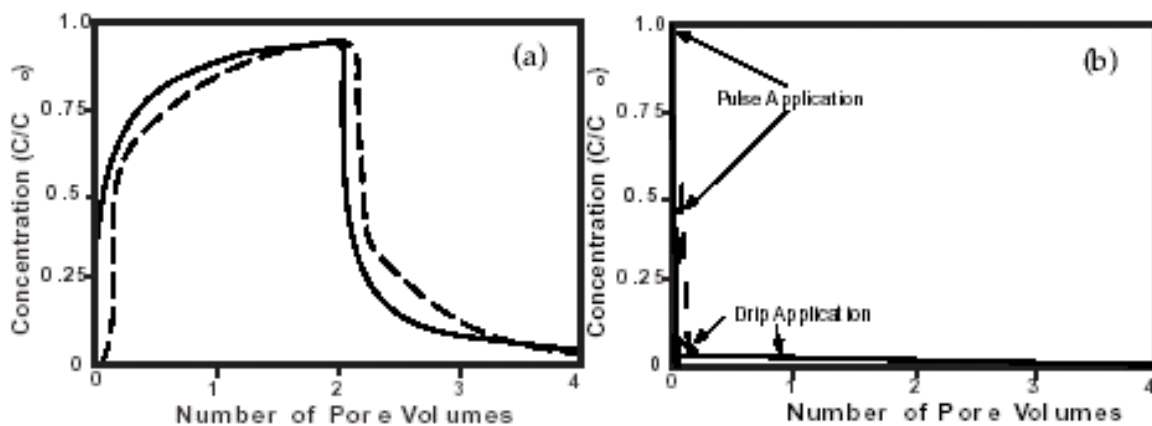


Figure 7. Predicted (dashed lines) and observed breakthrough (solid lines) curves for column A. (a) Ponded Application, and (b) Pulse and Drip Application. Data from Kluitenberg and Horton (1990).

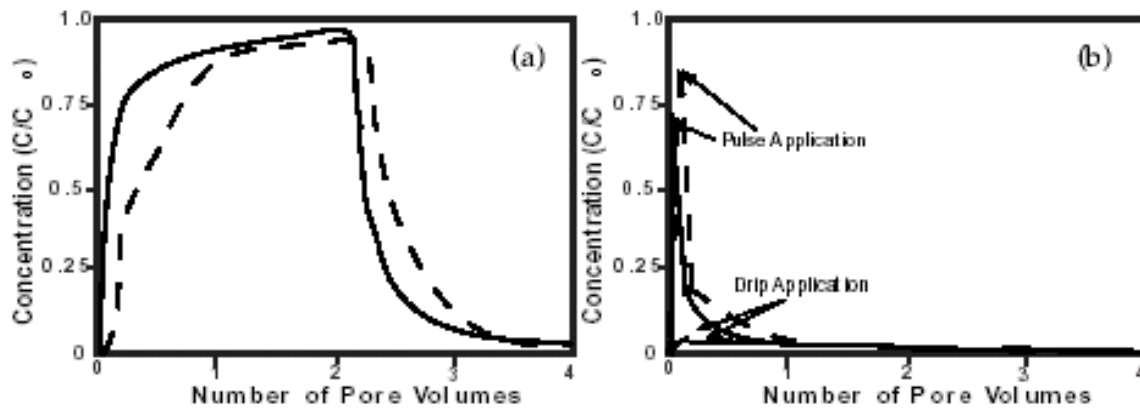


Figure 8. Predicted (dashed lines) and observed breakthrough (solid lines) curves for column B. (a) Pondered Application, and (b) Pulse and Drip Application. Data from Kluitenberg and Horton (1990).

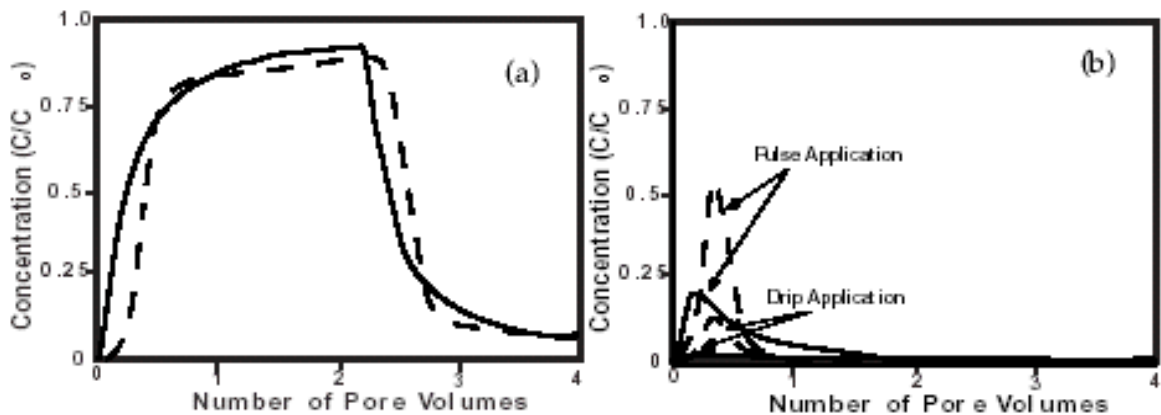


Figure 9. Predicted (dashed lines) and observed breakthrough (solid lines) curves for column C. (a) Pondered Application, and (b) Pulse and Drip Application. Data from Kluitenberg and Horton (1990).

References:

Anderson, J. L., & Bouma, J. (1977). Water movement through pedal soils: I. Saturated flow. *Soil Science of America Proceedings*, *37*, 408 - 413.

Anderson, J. L., & Bouma, J. (1977). Water movement through pedal soils: II. Unsaturated flow. *Soil Science of America Proceedings*, *37*, 419 - 423.

Barry, D. A. (1993). Modelling contaminant transport in subsurface: Theory and computer programs. In H. Ghadiri & C. W. Rose (Ed.), *Chapter 3, Modelling Chemical Transport in Soils: Natural and Applied Contaminants*. London. Lewis Publishers. 105 - 144.

Barry, D. A., & Li, L. (1994). Physical basis on nonequilibrium solute transport in soil. In *15th International Congress of Soil Science*, Acapulco, Mexico. 20 pp.

Barry, D. A., & Sposito, G. (1988). Application of the convective-dispersion model to solute transport in finite soil columns. Soil Science Society of America Journal, 52(1), 3 - 9.

Brooks, R. H., & Corey, A. T. (1964). Hydraulic properties of porous media. Hydrological Papers, No. 3, 27pp. Colorado State University, Fort Collins.

Charbeneau & S Charbeneau, R. J. (1981). Groundwater contaminant transport with adsorption and ion exchange chemistry: Method of characteristics for the case without dispersion. Water Resources Research, 17, 705 - 713.

Charbeneau, R. J. (1984). Kinematic models for soil moisture and solute transport. Water Resources Research, 20(6), 699 - 706.

Charbeneau, R. J., & Street, R. L. (1979). Modeling groundwater flow fields containing point singularities, streamlines, travel times, and breakthrough curves. Water Resources Research, 15(6), 1445 - 1450.

Gee, Kincaid Gee, G. W., Kincaid, T., Lenhard, R. J., & Simons, C. S. (1991). Recent studies of flow and transport in the vadose zone. (U. S. National Report of the International Union of Geodesy and Geophysics, 1987 - 1990), Reviews of Geophysics, 29, 227 - 239.

Gerke, H. H., & van Genuchten, M. T. (1993). A dual-porosity model for simulating preferential movement of water and solutes in structured porous media. Water Resources Research, 29, 305 - 319.

Kluitenberg, G. J., & Horton, R. (1990). Effect of solute application method on preferential flow transport of solutes in soil. Geoderma, 46, 283 - 297.

Li, Y., & Ghodrati, M. (1994). Preferential transport of nitrate through soil columns containing root channels. Soil Science Society of America Journal, 58, 653 - 659.

Nijssen, B. M., Steenhuis, T. S., Kluitenberg, G. J., Stagnitti, F., & Parlange, J.-Y. (1991). Moving water and solutes through the soil: Testing of a preferential flow model. In National Symposium on Preferential Flow, Chicago, Illinois. 223 - 232.

Parker, J. C., & van Genuchten, M. T. (1984). Determining transport parameters from laboratory and field tracer experiments. Bulletin, 84-3. Virginia Agricultural Experimental Station, Blacksburg.

Parker, J. C., & van Genuchten, M. T. (1984). Flux-averaged and volume-averaged concentration in continuum approaches to solute transport. Water Resources Research, 20(7), 866 - 872.

Parlange, J.-Y., Steenhuis, T. S., & Stagnitti, F. (1995). Percolation. In C. Finkl (Ed.), The Encyclopedia of Soil Science and Technology. Van Nostrand Reinhold.

Richard, T. L., & Steenhuis, T. S. (1988). Tile drain sampling of preferential flow on a field scale. Rapid and Far Reaching Hydrologic Processes in the Vadose Zone (Special Issue), Journal of Contaminant Hydrology, 3, 307 - 325.

Richards, L. A. (1931). Capillary conduction of liquids through porous mediums. Physics, 1, 318 - 333.

Skopp, J., Gardner, W. R., & Tyler, E. J. (1981). Two-region model with small interaction. Soil Science Society of America Journal, 45, 1147 - 1152.

Sposito, G., & Jury, W. A. (1988). The lifetime probability density function for solute movement in the subsurface zone. Journal of Hydrology, 102, 503 - 518.

Stagnitti, F., Steenhuis, T. S., Parlange, J.-Y., Nijssen, B. M., & Parlange, M. B. (1991). Preferential solute and moisture transport in hillslopes. In Challenges for Sustainable Development, Proceedings of International Hydrology and Water Resources Symposium, Institution of Engineers, Barton, Australia. 919 - 924.

Steenhuis, T. S., & Muck, R. E. (1988). Preferred movement of non-adsorbed chemicals on wet, shallow, sloping soils. Journal of Environmental Quality, 17, 376 -384.

Steenhuis, T. S., Nijssen, B. M., Stagnitti, F., & Parlange, J.-Y. (1991). Preferential solute movement in structured soil: Theory and application. In Challenges for Sustainable Development, Proceedings International Hydrology and Water Resources Symposium, Perth. Institute of Engineers, Australia. 3, 925 - 931.

Steenhuis, T. S., Parlange, J.-Y., & Andreini, M. S. (1990). A numerical model for preferential solute movement in structured soils. Geoderma, 46, 193 - 208.

van der Molen, W. H. (1956). Desalinisation of saline soils as a column process. Soil Science, 81, 19 - 27.